CERN – EUROPEAN ORGANIZATION FOR NUCLEAR RESEARCH

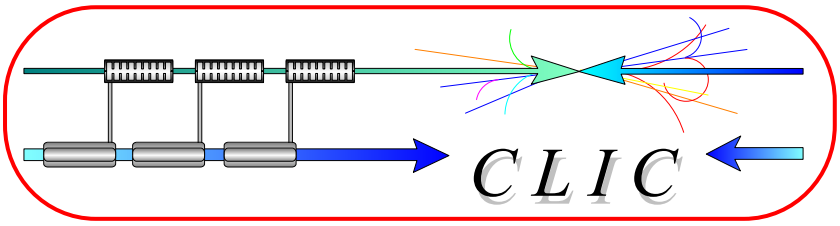

CLIC Note 590

CERN-OPEN-2004-002
09 February 2004

A NOVEL IDEA FOR A CLIC 937 MHZ 50 MW MULTIBEAM KLYSTRON

E. Jensen, P. Pearce, I. Syratchev

The CLIC study is based on 937 MHz, 50 MW, 100 μs Multi-Beam Klystron (MBK) with a design efficiency in excess of 65%. Unfortunately MBKs that meet the above specification are not currently available, and further design and development work will be needed to demonstrate that this specification can be achieved. An MBK is basically a parallel assembly of many low-current klystrons which use common RF structures for the interactions with the beams. Having a large number of beamlets in the klystron enables the power per beamlet to be considerably reduced leading to low current densities, low-perveance beams and hence high efficiency. A new MBK design concept is proposed, it is based on results and experience obtained from the use of Barrel-Open-Cavity (BOC) technology which was initially developed in Russia, but which has been developed further over the last few years at CERN. It is shown that this new concept leads to a multi-mode MBK design that is mechanically robust and simple to manufacture, with a possible efficiency of 80 %.

Geneva, Switzerland
09/02/2004

A NOVEL IDEA FOR A CLIC 937 MHZ 50 MW MULTIBEAM KLYSTRON

I. Syratchev[◊], *E. Jensen*, *P. Pearce*
CERN, Geneva

1. Introduction

There is a world consensus (ICFA, ECFA and ACFA) that the next large high-energy physics facility should be a TeV-range electron-positron linear collider. The feasibility of building a 3 TeV collider based on a two-beam scheme of acceleration (CLIC) is being studied at CERN for the post-LHC era [1]. This study requires a wide-ranging programme of accelerator research together with the design and development of state-of-the-art technologies. The CLIC study team is proposing high–power (~50 MW), long–pulse (~100 μs) 937 MHz multi-beam klystrons to supply the RF power needed to accelerate the low-energy, high-intensity drive beam. These klystrons should meet the minimum performance specification [2], given in Table 1. A multi-beam klystron (MBK) has been specified because it is believed that this is the only device that can achieve high efficiencies at these high powers.

Table 1. Multi-beam klystron (MBK) parameters for a 3 TeV linear collider

Parameter	Value	Units
Operating frequency	937.5	MHz
RF pulse width	100	μs
Pulse repetition frequency	100	Hz
Klystron peak RF power	50	MW
Klystron average power	500	kW
Efficiency	≥ 65	%
Gain at Saturation	≥ 43	dB
Beam voltage	< 220	kV

Multi-beam klystrons were developed in Russia and America in the mid–1960's [7]. An MBK is basically a parallel assembly of many low-current klystrons which use common RF structures for the interactions with the beams. Having a large number of beamlets in the klystron enables the power per beamlet to be reduced considerably leading to lower current densities and a very low perveance per beam. Beam perveance, defined as the current per beam divided by the 3/2 power of the voltage ($I_B/\sqrt{V^3}$) is a very important parameter which determines to a large extent the power conversion efficiency (this is explained in detail in section 2 below).

Unfortunately multi-beam klystrons that meet the above specification are not currently available, and further design and development work will be needed to demonstrate that this specification can be achieved.

This paper is a first step in this direction, and proposes a new MBK design concept. The new design concept is based on results and experience obtained [3,4] from the use of Barrel-Open-Cavity (BOC) technology which was initially developed in Russia, but which has been developed further over the last few years at CERN. As will be shown, this new concept leads to a multi-mode, MBK design that is mechanically robust and simple to manufacture, with a possible efficiency of 80 %.

[◊] This work is protected by the patent application PCT/EP03/14805.

2. Low perveance

Perveance characterizes the dependence of the current on the anode voltage in the regime of space charge limited (Child-Langmuir) emission, and it is approximately proportional to the (single) cathode area divided by the cathode-to-anode spacing squared. Optimization of the power conversion efficiency of a klystron *(η=rf output power/beam input power)* is closely linked [5] to drift length, beam radius and perveance as well as RF cavity tuning. The RF output current (and power), due to the input modulating voltage, is a maximum when the klystron transconductance g is a maximum *($g = I_{out}/V_{in} \propto b'/\sqrt{K}$ where b' is the normalized beam radius and K the perveance)*. It has been shown [6] that g is a maximum for an optimized beam radius when the perveance is a minimum. High efficiency klystrons (> 75 %) therefore require a low perveance. Since there is an upper technical limit to the voltage that can be applied, a low perveance can only be obtained by operating with low currents, and this for single beam klystrons is inconsistent with the need for high power. The idea of the MBK is to operate many low-current (low perveance) klystrons in parallel (using the same RF structures) to generate high power at high efficiency.

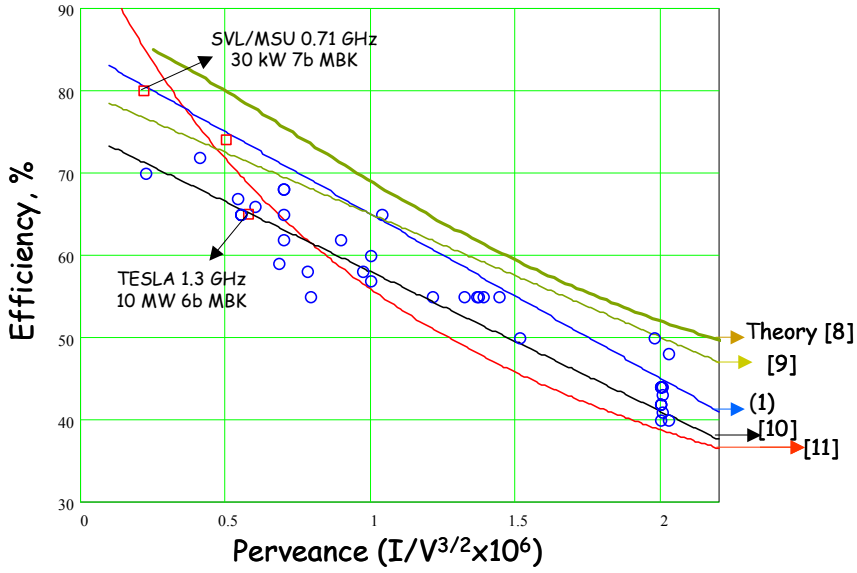

Figure 1: State-of-the-art single (circles) and multi-beam (rectangles) klystron efficiencies vs. single beam perveance.

Fig. 1 gives efficiency-perveance data for a selection of state-of-the-art klystrons for different frequencies and power levels. Many different fits for such data can be found in the literature [8-11], but the low-frequency, high-efficiency MBK data [12] is best fitted by the empirical law:

$$\eta = 0.85 - 0.20 \times \mu K \qquad (1)$$

This fit indicates that for very-low-perveance devices, efficiencies > 80 % are within reach. A similar conclusion was reached in [13] for the case of a gridded-gap (no fringe fields) conventional (non-relativistic) klystron with no space-charge effects, where studies predicted an efficiency as high as 90 %. It therefore seems reasonable to assume that such high efficiencies are indeed attainable for a low-frequency MBK with a large number of beamlets and hence a lower current per beam and a lower cathode voltage. Based on (1), the klystron output RF power for an MBK can be expressed as:

$$P = \eta I_b N_b V_b = (0.85 - 0.2 \times \frac{I_b \times 10^6}{V_b^{3/2}}) \times I_b N_b V_b \qquad (2)$$

where I_b is the single beam current (A), V_b – is the beam voltage (V) and N_b is the total number of beamlets. Fig. 2 gives the efficiency and single beam current versus number of beamlets for different cathode voltages for an output RF power of 50 MW.

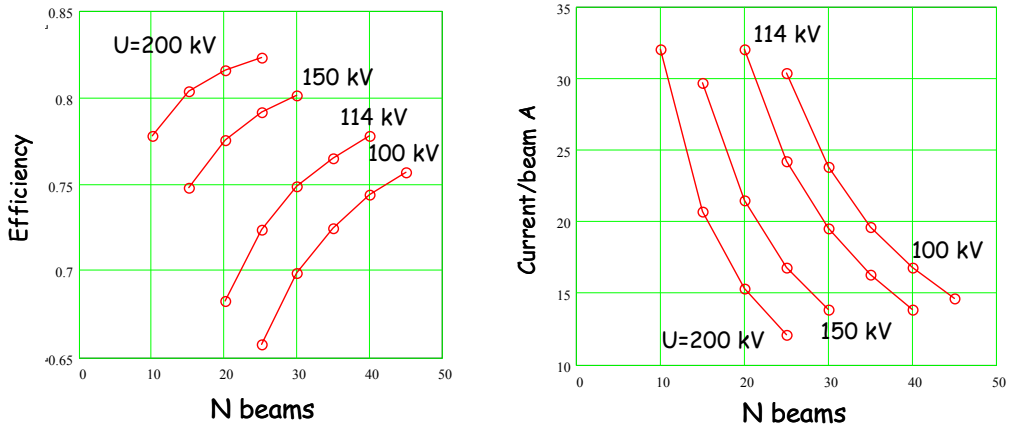

Figure 2: Efficiency and MBK's single beam current estimations vs. total number of beamlets for different cathode voltages.

If we target an efficiency of ~ 80 %, a beam voltage $V_b = 150\,\text{kV}$ seems reasonable for the design of the klystron modulator. Choosing 30 beamlets results in a single beam current of about 15 A.

3. MBK RF circuit

We have seen from Fig. 1 and Fig. 2 that to obtain a high efficiency MBK we require low perveance and that, to obtain high power we require a large number of beamlets. The number of beamlets and the design of the RF structures that can be used is, however, limited by geometric, RF and beam quality considerations. These include restrictions on the minimal distance between single beamlets coming from demands on cathode loading, the use of second harmonic cavities, space charge effects, the danger of exciting spurious mode instabilities and the overall size of RF cavities. The various designs to solve these problems that have been proposed over the decades since the first multi-beam klystron was developed are discussed in the following and are compared with a new CLIC MBK design proposal for the drive-beam accelerator. In this discussion we restrict ourselves to MBKs with common RF cavities. Cluster klystrons [9] and sheet beam klystrons [14] which are based on a similar line of thought are not considered here.

We will look at four different cases of field distributions in RF cavities that may be considered for use in an MBK (see Fig. 3). Cases 1 and 4 depict modes in a disc shape (radial) cavity, while cases 2 and 3 represent modes in an annular (waveguide type) cavity. These modes have very different *R/Q* values (*R/Q* gives the square of the voltage as seen by the beam for a given stored energy in the cavity). Fig. 4 shows the radial distribution of the axial electric field for all the cases.

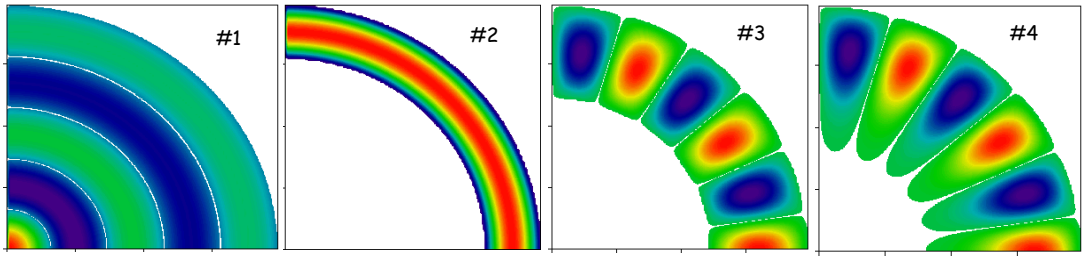

Figure 3: Different possible field distributions for MBK cavities.

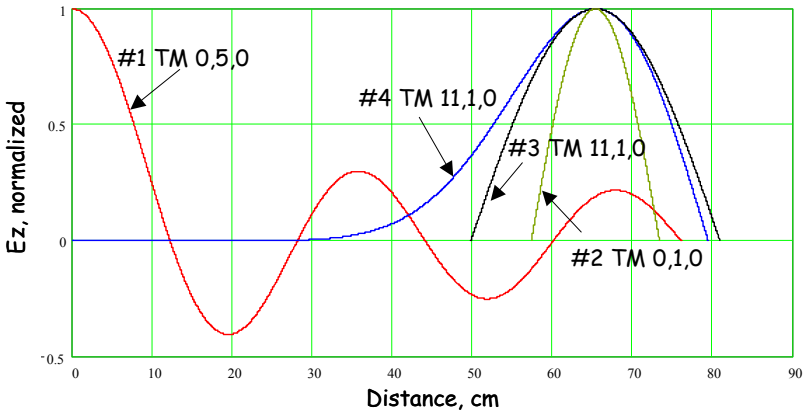

Figure 4: Radial distribution of the axial electric field for the different cases shown in Fig. 3.

The conventional MBK has a simple $TM_{0,1,0}$ (pillbox) cavity. The beamlets (typically between 6 and 30) pass through the cavity at different angular (and possibly also different radial) positions, close to the central maximum of the axial electric field. With these devices, very high efficiencies (80 %) have been demonstrated [12], but they have been achieved for relatively low RF power levels (tens of kW). Getting a higher power out of this device would require an increase in the beam current, which for this geometry is soon limited by both space charge effects and cathode loading. One way around this limitation is to change the operating mode of the cavity to a higher radial index mode (case 1). The TESLA 1.3 GHz, 10 MW, 6–beam MBK for example, uses the $TM_{0,2,0}$ mode [15] (compare Fig. 3, #1). Another way was studied by the Stanford Linear Accelerator Center (SLAC) for a 1.5 GHz, 2 GW, 10-beam MBK [16]. The design was based on the lowest mode of a ring cavity (see Fig. 3, #2). The same scheme was also studied, but eventually abandoned by Calabazas Creek Research for their 50 MW, X-band, 8-beam MBK [17]. Finally, a 150 MW, X-band, 6-beam MBK was proposed by KEK [18], based on a $TM_{12,1,0}$ waveguide mode (see Fig. 3, #3). The CLIC 50 MW, 937 MHz design is based on a high-azimuthal-order $TM_{m,1,0}$ mode in a disc-shape cavity and has 27 beams (see Fig. 3, #4). In this device the total number of beamlets is equal to about twice the index m of the operating mode. If we try to design a 27-beam MBK using the TESLA approach, we would have to work with the $TM_{0,5,0}$ mode. A major disadvantage here is the drastic drop of R/Q due to the energy stored in that part of the cavity that does not interact with the beam. To keep R/Q high, we need the energy to be stored only around the beam interaction area, as for example in cases 2 to 4. The R/Q's for cases 1 and 4 are compared in Fig. 5. For a given gap length and voltage, the impedance ratio is simply the inverse ratio of stored energies normalized to the individual Q-factor of each. One can see that starting already from n =3 the $TM_{m,1,0}$ (m =11) is more efficient than $TM_{0,n,0}$.

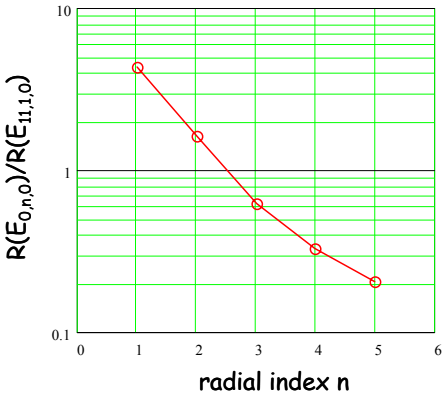

Figure 5. $TM_{0,n,0}$ interaction impedance vs. radial mode index n *normalized to the $TM_{11,1,0}$ mode impedance.*

Another very important issue for an MBK design is the parasitic mode spectrum. A strong damping of higher-order modes (HOMs) is absolutely necessary. During operation, the currents of individual beamlets will not in general be exactly balanced, and there will be a danger that any parasitic mode that has a corresponding angular current profile, or a parasitic-mode frequency close enough to the operating one, will be self-excited. It is clear that this problem will be particularly serious for case 1 where it is difficult to apply any damping technique and for case 2 because the operating mode is at the cut-off frequency of the waveguide, resulting in a very dense HOM spectrum.

Based on the above, it would seem that cases 1 and 2 have serious limitations for high-power applications, and in consequence we will limit further discussion to cases 3 and 4. A comparison of the impedances of $TM_{m,1,0}$ modes shows that for azimuthal indices around 10, the impedances for both cases are identical. Fig. 6 shows the frequency spectra within a ± 30 % frequency band. One can see that, as expected, the disc cavity has a much denser spectrum compared to the ring cavity. Although we are trying to keep the design as simple as possible, it should be mentioned that interaction strengthening via "nose cones", i.e. a capacitive rim near the maximum of the electric field, seems appropriate. In this case, the ring-cavity spectrum will certainly become denser since cutoff frequencies will be lowered. There seems to be no easy way to damp the HOMs of the ring cavity, since damping must be non–resonant; this is why measures like choke trapping, etc. do not apply. On the other hand, the field pattern of the operating mode in a disc cavity provides a natural way to achieve damping of unwanted parasitic modes.

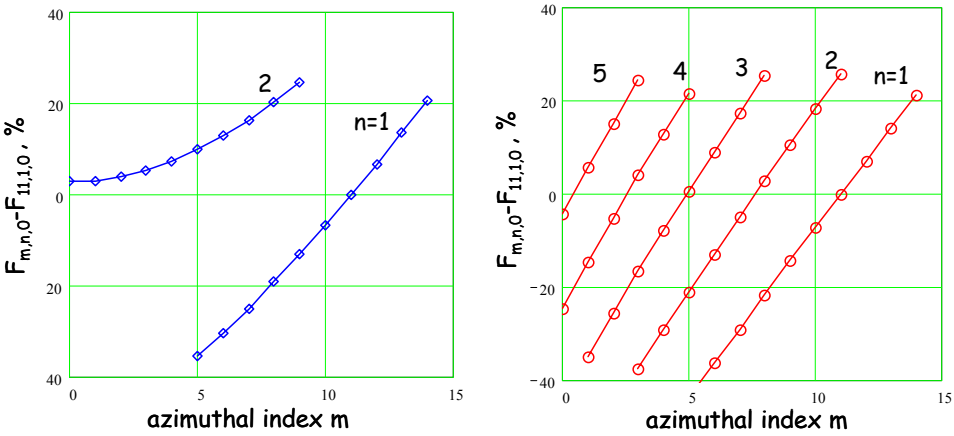

Figure 6: Mode density normalized (left –ring cavity, right – disc cavity)

It is a well-established fact that in the Barrel-Open-Cavity (BOC), which is used for high frequency RF pulse compressors [3, 19], the mode spectrum of $TM_{m,n,q}$ modes with large m ("*whispering gallery*" modes) can easily be made extremely sparse. All modes in the BOC with low-azimuthal index or high-radial and high-axial indices radiate efficiently through the open cavity faces, while the whispering gallery modes remain unaffected - see for example the X-band BOC spectra for closed and open faces shown in Fig. 7 [19].

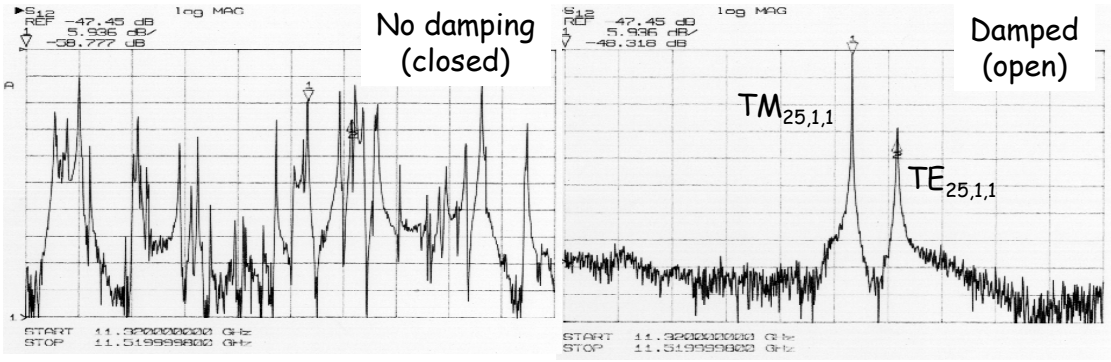

Figure 7: Measured spectra of an X-band BOC cavity.

For the disc cavity, the "open face" conditions may be replaced by an RF absorber which can be placed inside at a radius where the operating mode is virtually not affected. Experience gained with the 3 GHz BOC RF pulse compressor for the CLIC Test Facility 3 (CTF3) [20] confirms the validity of this approach. Simulations of a damped disc cavity geometry have been made using HFSS. The SiC absorber ring was placed at a position which produced a 10 % reduction of the operating mode Q–factor from 3.3×10^4 to 3.0×10^4. The Q-factors of all modes with a radial index higher than 3 were reduced by a factor of more than 1000 in the frequency band investigated. The damped Q-factors for modes with radial indices 1, 2 and 3 (normalised to their undamped values) are shown in Fig. 8. We assume that a Q-factor reduction of about 100 is enough to eliminate any effects on the beam. Using this assumption, we obtain the modified spectrum of the Damped Disc Cavity (DDC) shown in Fig. 9, the shaded area shows the modes that are no longer considered to be troublesome. It can be seen that the DDC provides a better performance than the ring cavity (cf. Fig. 9 and Fig. 6).

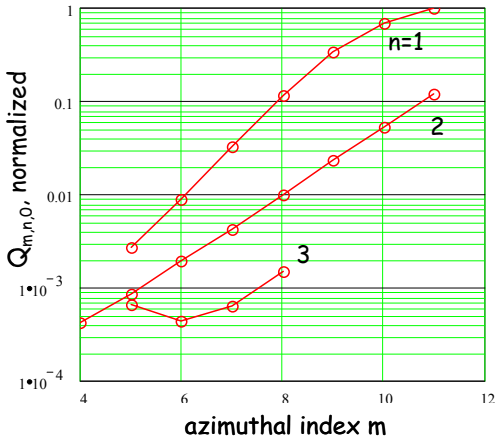

Figure 8: DDC Normalized HOM Q-factors.

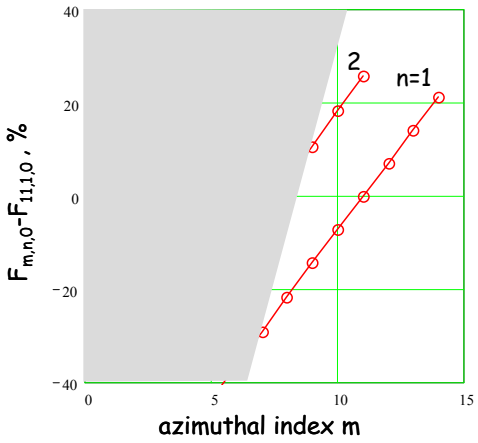

Figure 9: DDC modified spectrum.

A detailed DDC specification and design is outside the scope of this paper, which only presents the general DDC concept and points out some additional benefits that could be useful in a

final design. A general view of the DDC is shown in Fig. 10. The beam pipe diameter is rather small (~ 1/16 of the operating wavelength) and takes advantage of the low single-beam current and low frequency (see Table 2 below). As a result the fringe fields decay very rapidly resulting in a quasi-rectangular longitudinal electric field distribution, see Fig. 11. Also the electric field remains very constant, within 0.1 %, across the beam waist (λ/32). One can see that to some extent (viewed by each single beam), the DDC behaves like a gridded gap.

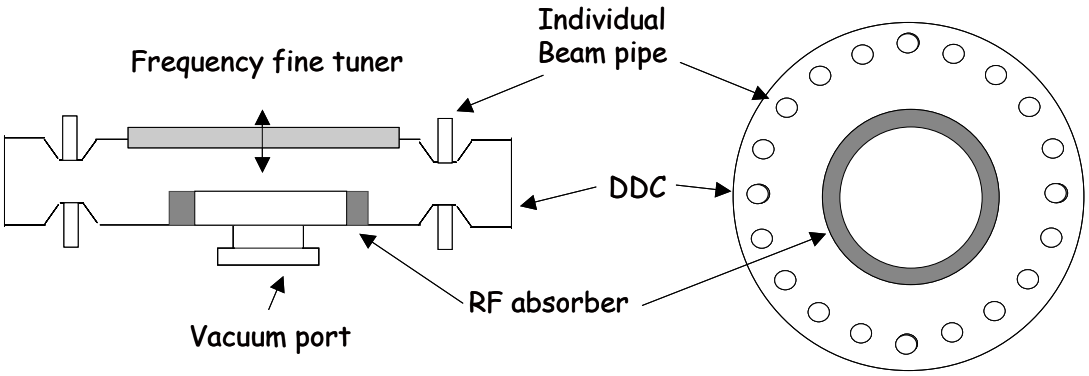

Figure 10: General view of the DDC.

The inter-beam space charge effects are minimized by the fact that the transverse beam spacing in a cavity is about half a wavelength (~ 16 cm). A good level of vacuum is necessary (10^{-8} mbar or better) to avoid beam instabilities due to ionization of residual gas [16]. The DDC, unlike the other geometries, can be very well pumped by mounting a high vacuum conductivity port (diameter ~ 40 cm) on the central part of the cavity as is shown in Fig. 10. For the gain cavities, the cavity impedance can be adjusted to the required value by a careful dimensioning of the RF absorber. The fine-tuning of the cavities should be done as shown in Fig. 10.

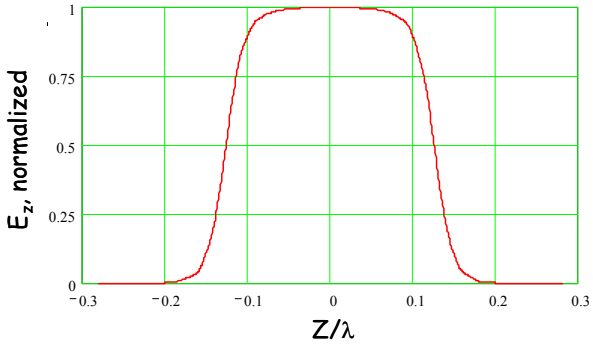

Figure 11: Longitudinal electric field distribution on a single beam axis.

A new feature of the CLIC design concerns the DDC regime of operation. Klystron cavities normally operate in a standing wave (SW) regime. In some devices [21, 22] the output cavity is a traveling-wave structure section where energy propagates in the longitudinal direction. With the DDC (and with a ring cavity) we can establish a new – resonant rotating wave (RW) regime, which is in fact a superposition of two standing waves shifted in space and time by a quarter of a period. The resulting wave travels along the outer cavity wall in a rotating mode. Complex amplitudes of the DDC electric field for the SW and RW regimes are shown in Fig. 12. The RW regime is very similar to that used in BOC systems [3].

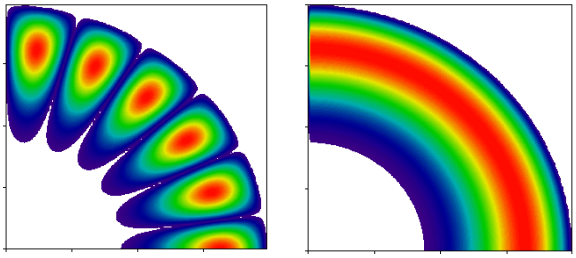

Figure 12: Plots of complex amplitudes of the DDC electric field for SW (left) and RW (right) regimes.

The RW regime brings certain advantages. First of all, the number of beamlets is decoupled now from the azimuthal index of the operating mode and can be arbitrarily chosen, as with the $TM_{0,n,0}$ mode. Moreover it is advisable that the number of beamlets chosen is odd so that the coupling of beam current to the modes that have closest azimuthal indices will be additionally reduced. As an example see Fig. 13, where we compare two regimes in terms of efficiency for the case of a 50 MW, 150 kV MBK, using the efficiency-perveance fit that was introduced before (1). The limit on the transverse spacing of the beamlets, for the case of the RW regime, was given by the size of the single $TM_{0,1,0}$ second harmonic cavity. Compared to SW, the RW regime, for the same operating mode, has reduced the single beam current by 25 %, so ensuring a higher efficiency.

During high power operation of the 3 GHz BOC pulse compressor, we found no traces of multipacting. This comes from the fact that with a pure traveling wave operation there are no closed trajectories for secondary electrons.

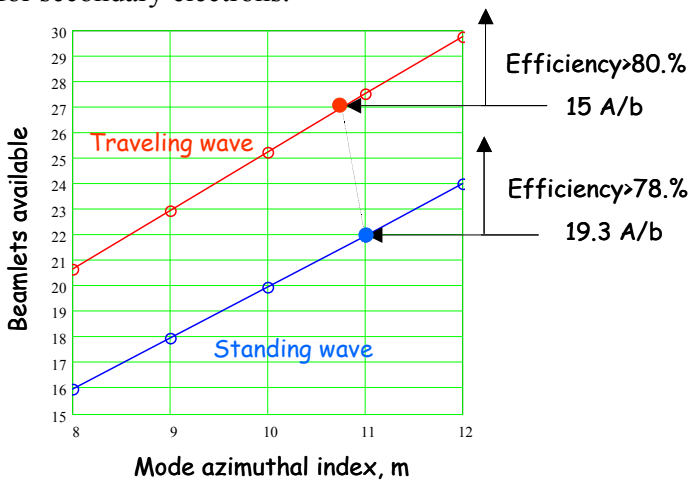

Figure 13: Comparison of RW vs SW efficiencies.

Coupling to the input and output cavities is done in a similar way to the BOC. The rectangular waveguide runs around the entire cavity. The cut-off frequency of the feeder (waveguide width) is chosen such that the phase velocities of the waves in both the waveguide and the cavity are identical at the operating frequency. Coupling to the cavity is made through many small coupling holes in the wall between the cavity and the waveguide. The best matching to the cavity is obtained when the distance between coupling holes is equal to a quarter of the operating mode wavelength - the total number of holes is therefore $4\times m$. The electric field plot in the cavity, simulated with HFSS, is shown in Fig. 14 (see also Fig. 15). Such a configuration provides a good matching to the cavity and reduces the probability of breakdown – the 3 GHz BOC cavity was processed up to 80 MW without any serious breakdown problems [20].

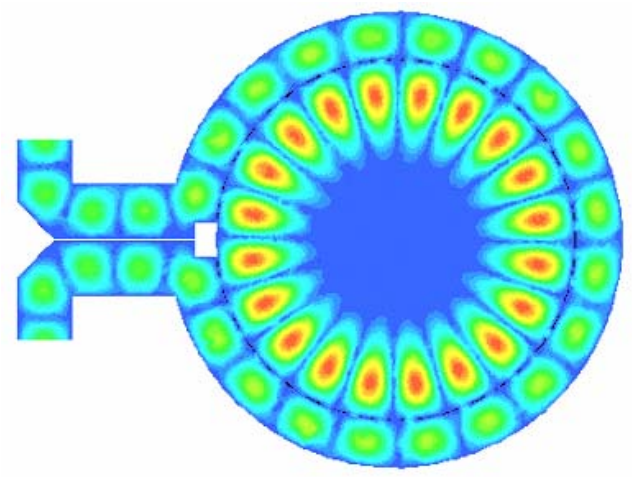

Figure 14: Electric field plot in a BOC median plane, operating in RW regime.

If the SW regime is chosen, the output waveguide port will have to be shortened and the number of coupling holes reduced to $2\times m$. This is necessary to fix the azimuthal orientation of the mode. In this case, the coupling (impedance) of the cavity can be adjusted by simply changing the position of the RF shorting stub. This provides a means for fine-tuning the klystron extraction efficiency.

4. Multi-Megawatt Mini-Windows concept

Klystron ceramic output windows are probably the most delicate RF components in the whole system. SLAC S-band klystron failure statistics for 10 years for example, showed that about 25 % of all klystron malfunctions were caused by RF window breakdown [23]. In the CLIC case, the design of a high peak power (50 MW) and high average power (0.5 MW) RF window would be considered very challenging. There have been a few recent innovations and developments in this area, like the H_{01} window [17, 24], mixed-mode traveling-wave window [25] and others. Scaling these solutions to our low frequency result in extremely large windows (typically about 0.5 m diameter) that would represent challenges to braze during fabrication and to cool during operation. Here again we are proposing a new Multi-Megawatt, Mini-Windows concept that exploits the properties of the DDC operating mode. The window layout is shown in Fig. 15.

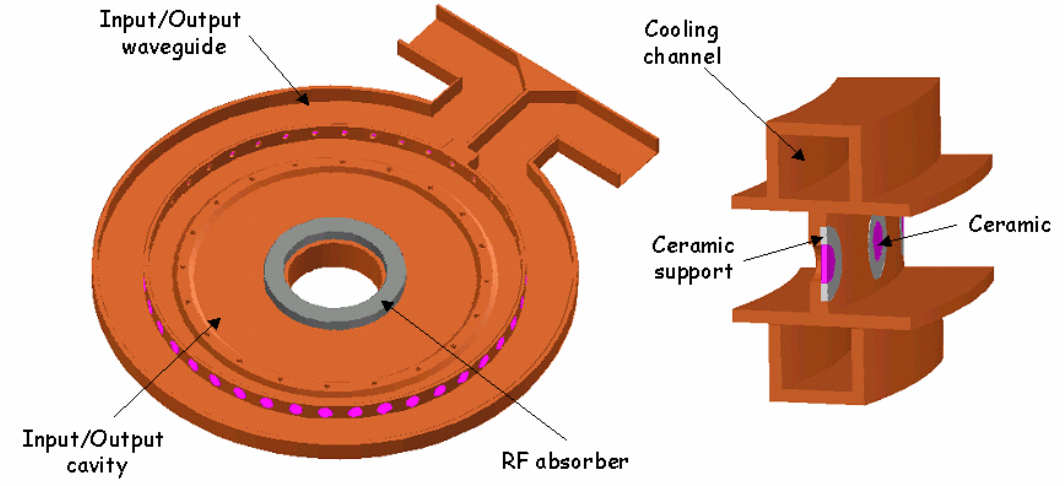

Figure 15: Artistic view of the output cavity with incorporated mini-windows.

The "window" is in fact a series of many mini-windows, each covering an individual coupling hole as shown in Fig. 15. The single mini-window is first brazed into its own support and then is electron-beam welded, or even clamped, into the inner wall of the waveguide. Typical dimensions of the ceramic disc are 2 mm thickness and about 30 mm diameter. The DDC field configuration is such that there is no notable electric field at the mini-window location. In the RW mode, with $4\times m$ mini-windows, the local power flow density will be reduced dramatically. For example with m = 11 and P = 50 MW, only 1.14 MW will be transferred through each window. As a result, we can expect high reliability.

5. Focusing system

Following the MBK RF configuration, a system of individual solenoids for each beamlet seems well suited to the design. A focusing magnetic field of 600 G to 700 G will be needed to steer each 150 kV, 15 A beam. A conventional solenoid will require about 1 kW per beamlet and this will reduce the overall klystron efficiency. The alternative choice is to use PPM focusing methods, similar to those proposed for the SLAC 1.5 GHz MBK [16].

6. Second harmonic cavities

Second harmonic cavities are normally used to improve the quality of the electron bunching and, in consequence, the klystron efficiency. This is quite common practice for any high efficiency klystron (see [26] for example). In our case we plan to use a set of individual $TM_{0,1,0}$ second harmonic cavities interacting with every single beamlet, as shown in Fig 16.

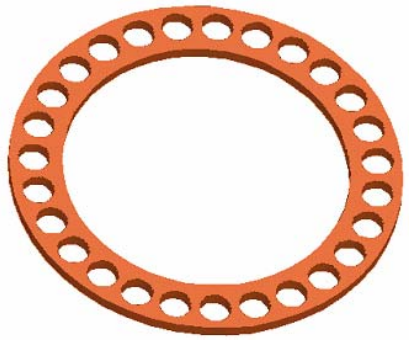

Figure 16: Artistic view of the common block of second harmonic cavities for 27 beamlets.

7. Cathode specification

The current density is the parameter that defines the cathode configuration. It is exponentially proportional to the temperature, and also inversely proportional to the exponential of the work function of the cathode material [Richardson-Dushman equation]. To keep beam compression as low as possible we would like to increase cathode loading, but this would increase the surface temperature and reduce the lifetime. Oxides of alkaline earth metals such as barium and strontium are added to the tungsten cathode to reduce operating temperatures. The lifetime of a klystron is primarily determined by cathode end-of-life emission, a result of barium depletion at the cathode surface. Cathode lifetime as a function of current density is given in Fig. 17 – this is based on a compilation of measured data taken over the past 30 years [15]. A cathode current density of 2 A/cm^2 was chosen (the same as the TESLA MBK proposal) because this potentially provides 145'000 hours of operation.

The parameters that define the gun-cathode assembly are beam voltage, beam current and beam diameter at the waist point in the klystron. These in turn help to determine the current density at the cathode for a desired lifetime as shown above. Preliminary calculations have been made using these four parameters to define a suitable Pierce Gun [27]. In these calculations, the cathode spherical diameter was compensated for spherical aberration effects [28], and particular attention was paid to finding an optimised beam convergence angle. Table 2 gives a first estimate of the parameters of an individual CLIC MBK gun-cathode structure resulting from these calculations.

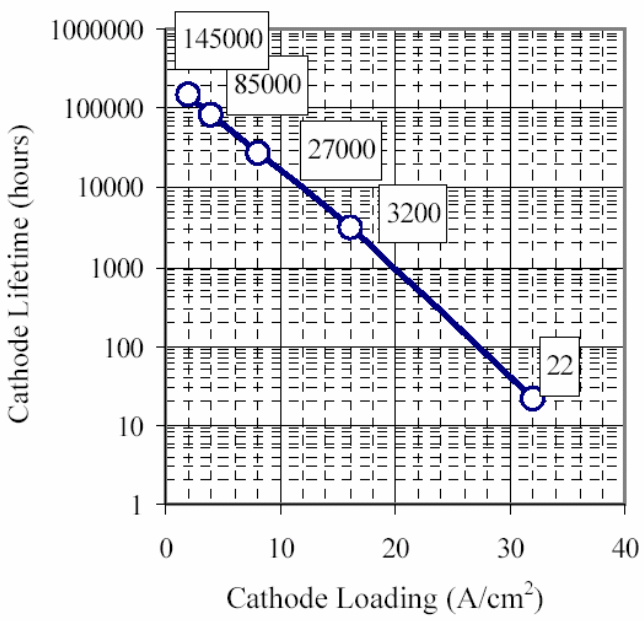

Figure 17: Lifetime versus loading for M-type dispenser cathode, space-charge-limited operation, 40 ^{0}C above the knee, picture taken from [15].

Table 2. CLIC MBK's single cathode preliminary parameters

Parameter	Value	Units
Beam voltage	154	kV
Beamlet beam current	15.04	A
Cathode current density	2	A/cm^2
Waist point beam radius	0.55	cm
Gun perveance×10^6	0.25	A×V$^{-3/2}$
Beam area compression ratio	8:1	-
Cathode disk radius	1.547	cm
Beam convergence half angle	10.75	degrees
Cathode spherical diameter	8.28	cm
Beam throw-cathode vertex to beam waist	12.5	cm
Maximum electric field level	35	kV/cm
Beam pipe diameter	2.0	cm
Confined flow focusing field	600-750	G

8. Collector

Since the klystron has been conveniently divided up into separate beamlets that can be considered as stand-alone klystrons in parallel, we could consider using individual collectors for

each beamlet. However, the cooling of such a device becomes complicated when about 30 small collectors are connected up in parallel to a common water supply and this also appears to be expensive to manufacture. The important design parameters for the collector are the mean and peak power to be dissipated, and the surface area on which the electron beam impinges. The minimum amount of cooling water (turbulent flow) required is generally estimated as 3 liters/minute for each kilowatt of average RF power dissipated. A large common collector (see Fig. 18), with each beam passing through its own pole piece at the output end of the tube, and allowed to expand in this magnetic-field-free region, would seem a more rational approach.

9. MBK layout

The overall gain (the ratio of peak output power to input drive power) will determine the minimum number of cavities that will be required. The CLIC bandwidth requirement is small (typically ± 3 %) so that we can assume that all gain cavities are tuned to approximately the same fundamental frequency and not stagger tuned. A second harmonic cavity is used to improve the bunching efficiency. Commercially available solid-state RF amplifiers are available at this frequency as input power source, and can reliably produce 300 W. An overall gain of 53 dB is then required from the klystron RF structures to develop the 50 MW peak power at the output. The klystron would then typically consist of 5 cavities: an input cavity, two gain cavities, a second harmonic cavity and an output cavity. A possible configuration for the CLIC multi-beam klystron is shown in Figure 18.

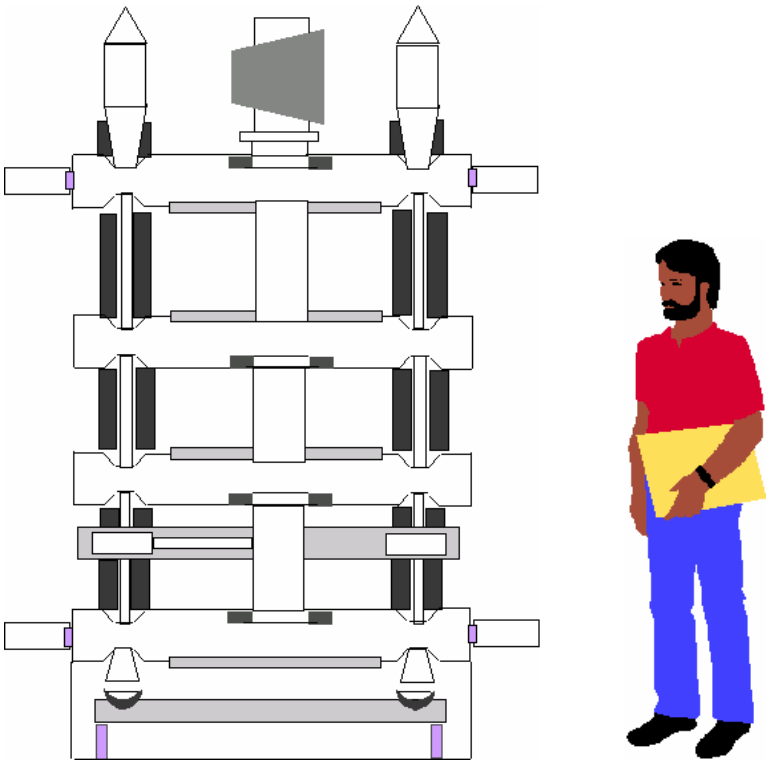

Figure 18: General layout of CLIC 0.937 GHz, 50 MW MBK.

10. Super MBK option

We have shown that the CLIC MBK design proposal consists of 27 individual mini-klystron sectors, each of which produces about 4 % of the total power obtained from the common

output cavity. Each single sector can in fact be treated as an individual device. If now, instead of using a single beamlet in this sector (Fig. 19, 1), we use a few mini-beamlets such that each sector acts like a mini MBK, we end up with a Super MBK (SMBK). Of course, the magnetic system as well as the second harmonic cavity would have to remain unique for every mini MBK. To make such a SMBK work we would have to modify the configuration in one of two ways. The first way would be to use a beam pipe with a larger radius, which can house a few mini-beams. In this configuration the annular beam can also be considered as a very good candidate, but unfortunately the second harmonic cavity becomes rather inefficient. The second way is to use a few individual beam pipes for each sector, see Fig. 19, 2) and 3) for example. Obviously, the RF power to be produced by each mini MBK is rather small. This is why we can use a very compact transverse arrangement of the mini-beamlets and a smaller beam pipe diameter. Through the optimization of each configuration, the electric field variation across the beam waist area was tuned to be less than ±3-4 %, keeping identical impedances along every single beam trajectory.

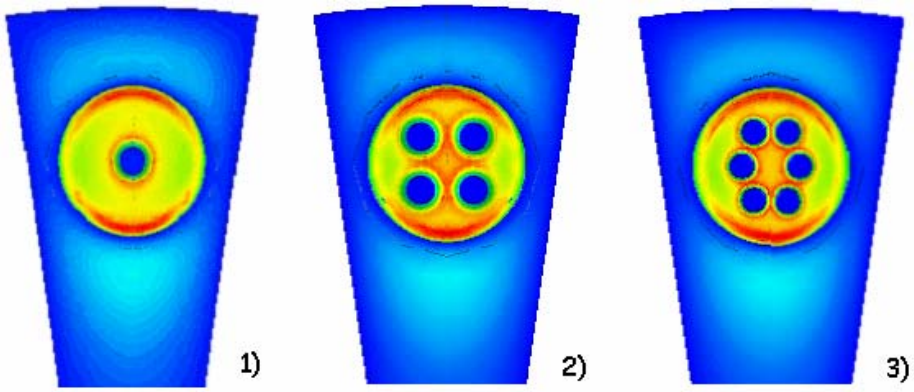

Figure 19: Different configurations of a mini MBK sector.

With the big number of beamlets ina SMBK, the RW regime becomes less attractive and so the SW regime was chosen for simplicity. With this regime a much improved HOM damping configuration can be considered, as shown in Fig. 20.

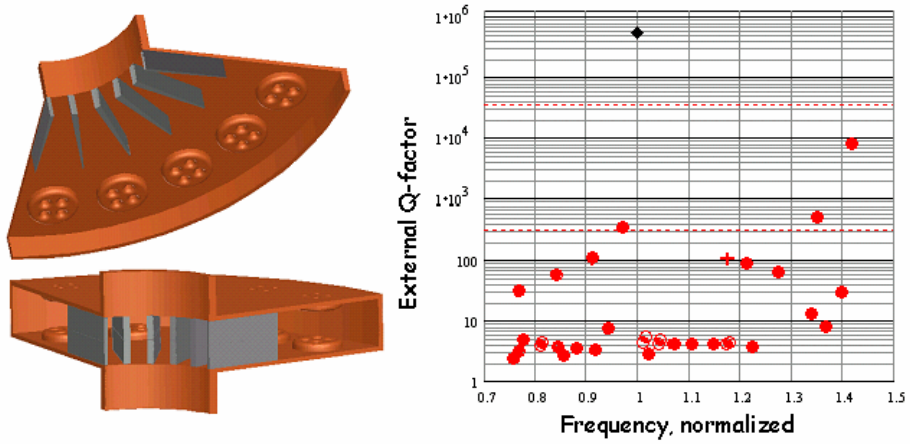

Figure 20. General view of the SMBK cavity and HOM damping performance.

Here, instead of using an absorbing ring (cf. Fig. 10), an array of many thin SiC wedges oriented towards the electric field minimums of the operating mode is proposed. The HFSS simulation results are presented in Fig. 20. In this picture the diamond indicates the operating mode external Q-factor due to the dielectric losses, the cross corresponds to the mode orthogonal

to the operating one, the circles show all the other modes that were found by HFSS, the upper broken line is the value of the unloaded Q-factor of the operating mode in a copper cavity and the lower one is its 1% level. Accepting a 100 times Q-factor reduction compared to the unloaded Q-factor of the operating mode as a safe limit (all the modes below the lower broken line), one can see that the nearest unwanted mode is about 40% higher in frequency than the operating one.

Another modification concerns the design of the second harmonic cavity of the SMBK. If this cavity is considered to be unique for each single sector, the standard pill-box cavity (Fig. 21, 1)) does not fit any more, because of the very strong electric field transverse asymmetry across the beam waist. As a solution we propose a coaxial, photonic-gap like cavity, as shown in Fig. 21 2. Using this approach the required symmetry of the electric field (rectangular in a given case) can be obtained with a proper choice of the arrangement of the outer posts. Electric field asymmetry across the single beam waist area in this case was calculated to be within a few percent.

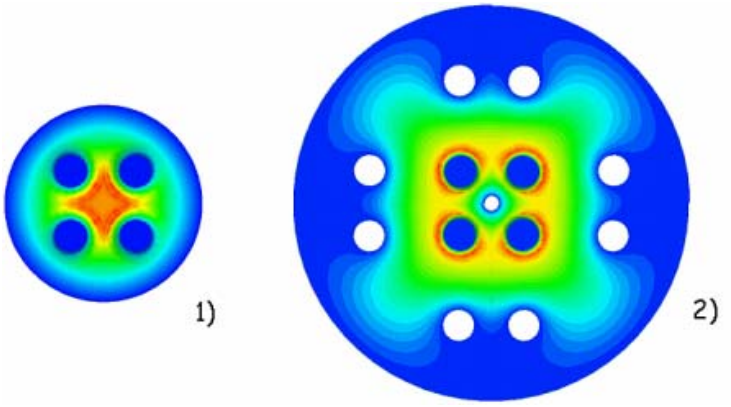

Figure 21. SMBK second harmonic cavity configurations.

Table 3. 50 MW MBK and SMBK parameters.

Parameter	MBK	SMBK#4	SMBK#6
RF power, MW	50	50	50
Beam Voltage, kV	167	96	81.5
R/Q along single beam line, Ω	143	90.4	87
Total current, A	376	653	768
Beamlets Number	22	22×4=88	22×6=132
Current/ beamlet, A	17.1	7.4	5.8
Power/beamlet, MW	2.86	0.71	0.47
Perveance×10^6	0.25	0.25	0.25
Cathode loading, A/cm^2	2.0	2.0	2.0
Single cathode area, cm^2	8.55	3.71	2.91
Beam compression ratio	9:1	3.9:1	4.2:1
Beam spot size, cm^2	0.95	0.95	0.69
Beam pipe diameter, cm	2.0	2.0	1.7
Steering magnetic field, G	600-750	500-600	400-500
Efficiency, %	80	80	80

The performances of the MBK and the SMBK with 4 and 6 mini-beamlets are compared in Table 3. We see from Table 3 that with the SMBK we can use a significantly lower cathode voltage and single beam current.

11. Modulators

The modulators that provide the long voltage pulse (~100 μs) for either a MBK or SMBK device will need to generate the same peak beam power. However, the beam voltage levels are different. If a classical modulator using a pulse transformer is considered then the lower voltage system should enable a faster rise time since less turns would be required on the secondary winding [29]. The pulse transformer would also be more compact due to the lower volt-seconds, and both leakage inductance and the self-capacitance of the windings would be reduced. This will improve the pulse response times and the energy efficiency by reducing the losses in the rise and fall of this voltage pulse. However, the voltage levels for both the MBK and SMBK are considerably lower than for an equivalent single beam klystron with the same output power, pulse width and duty cycle.

ACKNOWLEDGEMENTS

The authors would like to acknowledge I. Wilson for his enthusiastic support and encouragement as well as for many useful discussions and comments.

REFERENCES

[1] The CLIC Study Team: 'A 3 TeV e^+e^- Linear Collider based on CLIC Technology', CERN 2000-008, July 2000.
[2] P. Pearce: 'The L-band Klystron-Modulator RF power system for CLIC', IEE Pulsed Power 2000 Symposium, Digest No: 00/053, London, May 2000.
[3] Balakin V.E., Syrachev I.V.: 'VLEPP RF Power Multiplier', Proc. III-rd Int. Workshop on Next Generation Linear Collider, Branch INP, Protvino, Russia, 1991.
[4] I. Syratchev: 'RF pulse Compressors systems for CTF3', 5-th MDK Workshop, CERN, Geneva, 2001.
[5] T.G. Mihran: 'The effect of Drift length, Beam radius and Perveance on Klystron Power Conversion Efficiency', IEEE-ED, Vol. ED-14, No. 4, April 1967.
[6] Warnecke and Guenard: 'Tubes A Modulation Vitesse', Paris. Gauthier-Villars, 1951.
[7] E. Gelvich et al.: 'The new generation of high power MBK', IEEE-MTT, v. MTT-41, No. 1, 1993.
[8] R.S. Symons: 'Scaling laws and power limits for klystrons', IEDM, 1986.
[9] R.B. Palmer et al.: 'An immersed field cluster klystron', SLAC-PUB-5026, 1989.
[10] P.B. Wilson: 'RF power sources for 5-15 TeV linear colliders', Intern. workshop on pulsed RF sources for linear colliders, Shonan Village, Japan, April 1996.
[11] L. Harwood et al.: 'JLAB high efficiency klystron baseline design for 12 GeV upgrade', PAC 2003, Portland, Oregon, USA, 2003.
[12] A. Sandalov, V. Pikunov, V. Rodyakin: 'High efficiency conventional and relativistic klystrons', Intern. workshop on pulsed RF sources for linear colliders, Shonan Village, Japan, April 1996.
[13] Z.D. Farkas, P.B. Wilson: 'Dynamic of an electron in an RF gap', SLAC-PUB-4898 Rev, 1989.
[14] G. Caryotakis: 'A sheet beam klystron paper design', 5-th MDK Workshop, CERN, Geneva, 2001.
[15] E. Wright et al.: 'Development of a 10 MW, L-band multiple-beam klystron for TESLA', PAC 2003, Portland, Oregon, USA, 2003.
[16] G. Caryotakis et al.: 'Gigawatt multibeam klystron (GMBK)', 11th International Conference on High Power Particle Beams, Prague, Czech Republic, 1996.
[17] L. Song et al.: 'Development of a 50 MW Multi-Beam Klystron at 11.424 GHz', PAC 2003, Portland, Oregon, USA, 2003.
[18] A. Larionov, V. Teryaev, S. Matsumoto, Y.H. Chin: 'Design of multi-beam klystron in X-band', KEK-PREPRINT-2002-68, 2002.
[19] Syrachev I.V., Vogel V.F., Mizuno H., Odajiri J., Otake Y., Tokumoto S.: 'The Results of RF High Power Tests of X-Band Open Cavity RF Pulse Compression System', Proc. Int. Conference Linac-94, Tsukuba, Japan, 1994.
[20] P. Brown, private communication.
[21] G. Caryotacis: 'Development of X-band klystron technology at SLAC', PAC 97, Vancouver, Canada, 1997.
[22] T. Shintake et al.: 'Development of C-band 50 MW pulse klystron for e^-e^+ Linear Collider', PAC 97, Vancouver, Canada, 1997.
[23] P.B. Wilson: 'Advanced RF power sources for linacs', Linac 96, Geneva, Switzerland, 1996.

[24] W.R. Fowkes et al.: 'Recent advances in high power windows at X-band', High Density Microwaves, AIP Conf. Proc. 474, Pajaro Dunes, CA, 1998.
[25] S. Yu. Kazakov: 'High Power Testing Results of the X-Band Mixed-Mode RF Windows for Linear Colliders', Linac 2000, Monterey, CA, 2000.
[26] V. Kanavets, O. Pavlov, A. Sandalov: 'Stratification effect and maximum efficiency of a multi-cavity power klystron', SLAC-TRANS-0179, Nov 1977. 20 pp. Translated from the Russian Journal Elektronnaya Tekhnika, Ser.1, No.3, pp. 13-24, 1974.
[27] J.R. Pierce: 'Theory and Design of Electron Beams', Van Nostrand, New York, 1950, pp 182-192.
[28] R.D. Frost and O.T. Purl: 'Research on electron guns for intermediate and high power traveling wave tubes', Watkins-Johnson Co., ASD rep. ASD-TR-61-635, Sept. 1962.
[29] P.B. Wilson: 'Development and advances in conventional high power RF systems', SLAC-PUB-95-6957.